Comparison of GC–MS and NMR for Metabolite Profiling of Rice Subjected to Submergence Stress

ARTICLE *in* JOURNAL OF PROTEOME RESEARCH · DECEMBER 2012

Impact Factor: 4.25 · DOI: 10.1021/pr300953k · Source: PubMed

Journal of proteome research

Article

pubs.acs.org/jpr

Comparison of GC-MS and NMR for Metabolite Profiling of Rice Subjected to Submergence Stress

Gregory A. Barding, Jr.,[†,‡] Szabolcs Béni,[†,§] Takeshi Fukao,[‡,∥,⊥] Julia Bailey-Serres,[‡,∥] and Cynthia K. Larive*[,†,‡]

[†]Department of Chemistry, University of California—Riverside, Riverside, California 92521, United States

[‡]Center for Plant Cell Biology, University of California—Riverside, Riverside, California 92521, United States

[§]Department of Pharmaceutical Chemistry, Semmelweis University, Budapest, Hungary

[∥]Department of Botany and Plant Sciences, University of California—Riverside, Riverside, California 92521, United States

[⊥]Department of Crop and Soil Environmental Sciences, Virginia Tech, Blacksburg, Virginia 24061, United States

Supporting Information

ABSTRACT: Natural disasters such as drought, extreme temperatures, and flooding can severely impact crop production. Understanding the metabolic response of crops threatened with these disasters provides insights into biological response mechanisms that can influence survival. In this study, a comparative analysis of GC-MS and ^{1}H NMR results was conducted for wild-type and tolerant rice varieties stressed by up to 3 days of submergence and allowed 1 day of postsubmergence recovery. Most metabolomics studies are conducted using a single analytical platform. Each platform, however, has inherent advantages and disadvantages that can influence the analytical coverage of the metabolome. In this work, a more thorough analysis of the plant stress response was possible through the use of both ^{1}H NMR and GC-MS. Several metabolites, such as *S*-methyl methionine and the dipeptide alanylglycine, were only detected and quantified by ^{1}H NMR. The high dynamic range of NMR, as compared with that of the GC-TOF-MS used in this study, provided broad coverage of the metabolome in a single experiment. The sensitivity of GC-MS facilitated the quantitation of sugars, organic acids, and amino acids, some of which were not detected by NMR, and provided additional insights into the regulation of the TCA cycle. The combined metabolic information provided by ^{1}H NMR and GC-MS was essential for understanding the complex biochemical and molecular response of rice plants to submergence.

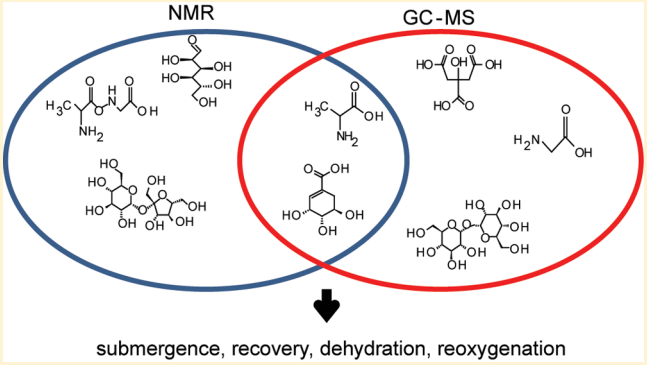

KEYWORDS: *metabolic profiling, metabolomics, submergence, recovery, reoxygenation, dehydration, rice, NMR spectroscopy, gas chromatography*

INTRODUCTION

Metabolomics is a rapidly growing field of research providing information downstream of genetic responses to biotic and abiotic stressors. Many metabolomics studies have been conducted with mammals to better understand human diseases[1] and in plant systems with the intent of improving disease resistance and crop production;[2] however, results have also been reported for fungi, bacteria, fish, and other organisms.[3−6] Because of the complexity of the samples interrogated, the analytical methods for metabolomics studies need to have both high resolving power and the ability to provide robustly quantitative results. Several analytical techniques have been used for metabolomics and metabolite profiling including capillary electrophoresis−mass spectrometry (CE-MS),[7] liquid chromatography−mass spectrometry (LC-MS),[8] gas chromatography−mass spectrometry (GC-MS),[6,9] and nuclear magnetic resonance (NMR).[10,11]

GC-MS using electron ionization is a popular analytical platform for metabolomics studies due to its sensitivity and reproducibility as methods are readily transferable between laboratories and instruments. The robustness of GC-MS measurements has largely been facilitated by the adoption of uniform MS parameters affecting fragmentation and through the use of retention indices that minimize discrepancies in the chromatography.[12] The inclusion of metabolite fragmentation patterns and retention index information into publicly available libraries has increased the utility of GC-MS for metabolomics studies of complex biological organisms.[13,14] GC-MS has been successfully used to query plants, fungi, mammals, fish, and amphibians for their metabolic response to a variety of biotic and abiotic stressors.[9] GC-MS is particularly effective in the analysis of primary metabolites, specifically those involved in central

Received: October 10, 2012
Published: December 3, 2012

carbon metabolism. To circumvent the low volatility of most biological compounds, prior to GC-MS analysis, molecules are silylated, and sugar cyclization is reduced through methoximation of ketones and aldehydes.[9] Because of extensive prior analytical method development, GC-MS is a popular and reliable analytical platform for the sensitive detection of a wide variety of metabolic classes. However, not all molecules are amenable to derivatization, and once derivatized, analytes are not all sufficiently volatile or stable for GC separations.

NMR is another widely used analytical platform for metabolite profiling because it is inherently quantitative, provides universal detection for organic compounds, and readily reveals structural information based on chemical shifts and coupling patterns. When a high-field magnet is used, NMR can often resolve the component resonances of mixtures of moderate complexity even without coupling to a separation technique. Additionally, NMR is readily adapted to a variety of sample formats (including both liquid and solid state samples),[15] is not restricted to hydrophilic or hydrophobic compounds, and typically has a better dynamic range than its time-of-flight (TOF)-MS counterpart.[16] For samples already in liquid form, such as urine, minimal sample preparation is required and the NMR measurements can be automated using an autosampler or flow probe for high-throughput analyses.[17] As with GC-MS, publicly available libraries of metabolites and their corresponding NMR spectra provide researchers access to tools for confident resonance assignments and inter/intralaboratory transferability.[13,18] However, NMR is not without disadvantages. Resonance overlap due to sample complexity can limit quantitation and identification; this can be especially problematic in serum or plasma samples where the high concentrations of lipids and proteins can obscure the resonances of the small molecule analytes of interest.[17] Despite significant improvements to sensitivity through the use of higher field magnets and the introduction of cryogenically cooled probes and receivers, for many metabolites, NMR is not as sensitive as MS-based methods. Because of the inherent advantages and limitations of GC-MS and NMR, both platforms were used in this study to query the metabolic response of two rice (*Oryza sativa* L.) varieties to submergence stress with the goal of critically comparing the strengths and weaknesses of each instrument.

Rice, a staple food crop, is often subjected to prolonged flooding events, resulting in stunted growth and death. The prevailing hypothesis regarding rice survival during submergence stress is centered on carbohydrate consumption.[19−21] Upon submergence, the phytohormone ethylene becomes entrapped, which in most rice cultivars, including *O. sativa* ssp. *japonica* cv. M202 used in this study, results in increased gibberellic acid (GA) responsiveness leading to carbohydrate consumption due to the elongation growth of aerial tissue.[19] This has been characterized as an escape strategy in which the plant consumes its carbohydrate resources in an attempt to grow above the water line and resume photosynthesis.[22] In contrast, the submergence tolerant variety *O. sativa* ssp. *japonica* cv. M202(*Sub1*) exercises a quiescence strategy in which the *SUBMERGENCE1A* (*SUB1*A) gene reduces the plant's responsiveness to GA, slowing carbohydrate consumption and shoot elongation. In addition to increased submergence tolerance, *SUB1*A-containing rice has also been shown to be better able to recover from drought stress by decreasing leaf water loss and increasing the expression of genes affiliated with drought adaptation.[23] Interestingly, upon desubmergence, rice plants undergo both reoxygenation and dehydration stresses; however, the effects of *SUB1*A on the metabolite profile during desubmergence have not been determined using GC-MS.[19,23]

We previously reported the results of a ^{1}H NMR metabolomics study of extracts of M202 and M202(*Sub1*) seedlings designed to probe metabolic reconfiguration as result of up to 3 days of complete submergence and during a 1 day postsubmergence recovery period. The NMR spectra of the intolerant M202 plants reflected the rapid consumption of sucrose following submergence.[24] As compared with the controls, initial glucose levels for the intolerant variety rose dramatically and then gradually decreased over the 3 day submergence. A corresponding increase in other metabolites associated with pyruvate and glucose metabolism including alanine (Ala), threonine (Thr), valine (Val), leucine (Leu), and other amino acids was also observed. These NMR results corroborate the increased carbohydrate consumption associated with the escape response of submerged M202 plants. In contrast, in experiments with the submergence tolerant M202(*Sub1*) variety, the extent of carbohydrate consumption and resulting amino acid accumulation was less dramatic, reflective of the quiescence strategy associated with rice varieties containing the *SUB1A* gene.

S-Methyl methionine (SMM) was identified in the ^{1}H NMR spectra of extracts of both rice varieties.[24,25] SMM levels decreased significantly over the course of the experiment, although no significant difference was observed for the two genotypes investigated. SMM has been implicated as a possible regulator of ethylene biosynthesis as well as in sulfur transport and methionine storage.[25−28] The ^{1}H NMR resonances of the dipeptide alanylglycine (AlaGly) were also detected in the spectra of extracts of both tissue types. Although no differences in AlaGly content were evident in the two varieties during submergence, the dipeptide was one of the more abundant metabolites detected. A GC-MS study of the metabolism of rice (*O. sativa* cv. Amaroo) embryos under aerobic and anaerobic germination conditions (dark, 30 °C) failed to report detection of either SMM or AlaGly.[29] The same report describes stress-induced changes of a variety of organic acids and tricarboxylic acid (TCA) cycle intermediates that were not detectable in our ^{1}H NMR experiments.[29] To rationalize the differences in metabolites reported in these two studies, this work compares the results of the independent yet complementary ^{1}H NMR and GC-MS techniques to profile the response of the commercially grown submergence intolerant M202 and the cross-bred submergence tolerant M202(*Sub1*) rice varieties under normal growth conditions, submergence stress, and recovery following submergence. Through a comparative analysis of both genotypes, a better understanding of the relative attributes of ^{1}H NMR and GC-MS for metabolomics studies can be discerned.

MATERIALS AND METHODS

Materials and Reagents

N-Methyl-*N*-trimethylsilyltrifluoroacetamide (MSTFA) in 1% trimethylchlorosilane for metabolite derivatization was purchased from Thermo Fisher Scientific (Waltham, MA). Fatty acid methyl esters (FAMEs) for retention index markers were purchased from Supelco (Sigma-Aldrich Corp., St. Louis, MO). Methoxyamine hydrochloride (MeOX) was purchased from Sigma-Aldrich. Metabolite standards were purchased from Sigma-Aldrich, Fisher Scientific (Pittsburgh, PA), and MP Biomedicals (Solon, OH). Water (18 MΩ/cm) was obtained using a Millipore filtration system (Millipore, Billerica, MA).

dx.doi.org/10.1021/pr300953k | J. Proteome Res. 2013, 12, 898−909

Pyridine (+99% purity) was purchased from Acros Organics (Thermo Scientific, West Palm Beach, FL). Chloroform, obtained from Mallinckrodt Laboratory Chemicals (Phillipsburg, NJ), and methanol (Fisher Scientific) were of at least ACS grade.

Growth Conditions and Plant Materials

O. sativa ssp. *japonica* cv. M202 and cv. M202(*Sub1*) were grown and stressed for up to 3 days to avoid tissue death as described by Fukao et al. and Barding et al.[19,24] Surface sterilization of the seeds was accomplished with 0.2% Tween-20 and 1% sodium hypochlorite, after which the seeds were rinsed thoroughly with deionized (DI) water. Seeds were soaked in the dark overnight in DI water and germinated on moist paper in a Pyrex dish covered with plastic wrap for 5 days. Germinated seeds were transplanted into 10 cm × 10 cm pots with soil (25 plants per pot) and grown until the three-leaf stage (12 days) at 30 °C in a greenhouse at ambient light. Transplanted seeds were fertilized with Peters Excel 21-5-20 liquid fertilizer. The seedlings had a survival rate greater than 99%.

Submergence Stress and Plant Harvest

Submergence stress was carried out in six 121 L trash cans containing DI water to minimize water salinity and equilibrated overnight to the ambient greenhouse temperature. Once the seedlings matured to the three-leaf stage, they were submerged for 0 (initial control), 1, 2, or 3 days or subjected to 3 days of submergence and 1 day of recovery. For the recovery sample, plants were desubmerged and placed for 24 h on the greenhouse bench prior to harvesting. Submerged plants were removed from the trash cans, and aerial tissue was immediately harvested, rinsed in DI water, flash frozen in liquid nitrogen, and stored at −80 °C. Control tissue was treated similarly, including a DI water rinse prior to flash freezing. Harvesting of all plants occurred at 1 p.m. Following harvest, samples were ground by mortar and pestle under liquid nitrogen to a fine powder, lyophilized overnight until dry, and stored at −80 °C. There were four biological replicates for each treatment, with each biological replicate consisting of a homogeneous tissue pool from the plants in one pot (n = 25). Aliquots of each tissue pool were also analyzed using ^{1}H NMR as reported previously.[24]

Tissue Extraction

Metabolite extraction was carried out using 10 mg dry weight of lyophilized tissue with modification of the previously described method.[24] Briefly, the dried tissue was extracted with 1.0 mL of 80/20 MeOH/H_2O extraction solvent in a 1.5 mL Eppendorf microcentrifuge tube. The samples were agitated for 1 min at 300 rpm using a platform shaker and centrifuged at 12000g for 4 min. A 50 μL aliquot of supernatant was transferred to a 350 μL glass GC flat bottom insert (Phenomenex, Torrence, CA) in a 1.5 mL Eppendorf tube and centrifuged under vacuum overnight using a Thermo-Savant SC110 model speed vacuum equipped with an RVT400 refrigerated vapor trap attached to a GP110 gel pump. Dried extracts were stored at −20 °C until derivatization for GC-MS analysis.

Sample Preparation

Dried metabolite extracts were treated according to Lee and Fiehn.[6] To each glass insert, 10 μL of 40 mg/mL MeOX in pyridine was added, and the sample was shaken at 30 °C for 90 min. This was followed by addition of 4 μL from a standard mixture of FAMEs of a linear carbon chain length C8, C9, C10, C12, C14, C16, C18, C20, C22, C24, C26, C28, and C30. The standard mixture of FAMEs was prepared in chloroform with a C8−C16 concentration of 0.8 mg/mL and a C18−C30 concentration of 0.4 mg/mL. Samples were allowed to react with 90 μL of MSTFA at 37 °C for 30 min, after which the glass inserts were transferred directly to a wide-mouth crimp top vial (Phenomenex) and sealed with an 11 mm crimp cap. Samples were analyzed within 24 h of derivatization.

Sample Injection and GC

An Agilent 7683B Automatic Liquid Sampler equipped with a 10 μL Agilent syringe (Agilent Technologies, Santa Clara, CA) was used to inject 1 μL of derivatized sample, after which the syringe was cleaned three times in methylene chloride in preparation for the next injection. The sample was injected into a splitless, single-tapered MS-certified injector liner with glass wool (Agilent Technologies) heated at 230 °C and changed every 25 samples to ensure efficient analyte transfer to the GC column. The injector was operated in pulsed splitless mode with helium (99.998% purity, CalTool, Riverside, CA) pressure ramped to 35.0 PSI for 0.5 min, after which the flow was reduced and maintained at 1 mL/min for the duration of the separation. The separation was carried out using an Agilent 7890A gas chromatograph equipped with an Rtx-5sil MS column, 0.25 mm i.d. and 30 m length with an additional 10 m integrated guard column. The sample was introduced at an initial oven temperature of 60 °C held for 1 min, ramped at 10 °C/min to a final temperature of 320 °C, and held for 5 min. The total run time was 32 min. All instrument operations were controlled by Waters MassLynx software version 4.1 (Waters Corporation, Milford, MA).

Mass Spectrometry Data Acquisition and Analysis

The sample was introduced from the GC to the MS at a transfer line temperature of 320 °C. Electron impact ionization was used at 70 eV with a source temperature of 220 °C. The filament was turned on after 6.5 min, and mass spectra were recorded from m/z 50 to 600 at a rate of 10 spectra s^{-1}. The detector was operated at 2700 V. An additional solvent delay was incorporated starting at 24.7 min and ending at 25.0 min to prevent ionization of sucrose, which is present at high abundance and would saturate the detector. Data were collected without the use of the dynamic range enhancement feature of the Waters GCT Premier to avoid compromising deconvolution and integration of the highly complex chromatograms. The data were collected and stored in Waters file format (*.raw). Data were converted as collected from Waters file format to *.cdf format for processing with the Automated Mass Spectral Deconvolution and Identification System (AMDIS, NIST, Gaithersburg, MD). Deconvolution settings used a component width of 17 scans, high resolution, high sensitivity, and medium shape. Retention indices (RIs) were calculated for each sample by AMDIS using an internal standard library and calibration standard library. For compound identification, AMDIS queried the NIST 08 Mass Spectral Library. All compound identities were confirmed with RI and MS data obtained from the Golm Metabolome Database or checked against an in-house library generated using metabolite standards.[14]

MarkerLynx XS (Waters Corporation) was used for data preprocessing to collect integration values for identified metabolites. Peaks were detected without smoothing from an initial retention time of 7.00 min and a final retention time of 32.00 min, with a low-mass cutoff of 73.5 Da, a high-mass cutoff of 600 Da, and a mass accuracy of 0.10 Da. The peak width at 5% was overestimated as 2 s to ensure peak detection. A peak-to-peak baseline noise value of 1.0, a marker intensity threshold of 25 counts, and a mass and retention time window of 0.1 Da/min were also used. A noise elimination level of 3.0 was chosen, and

dx.doi.org/10.1021/pr300953k | J. Proteome Res. 2013, 12, 898−909

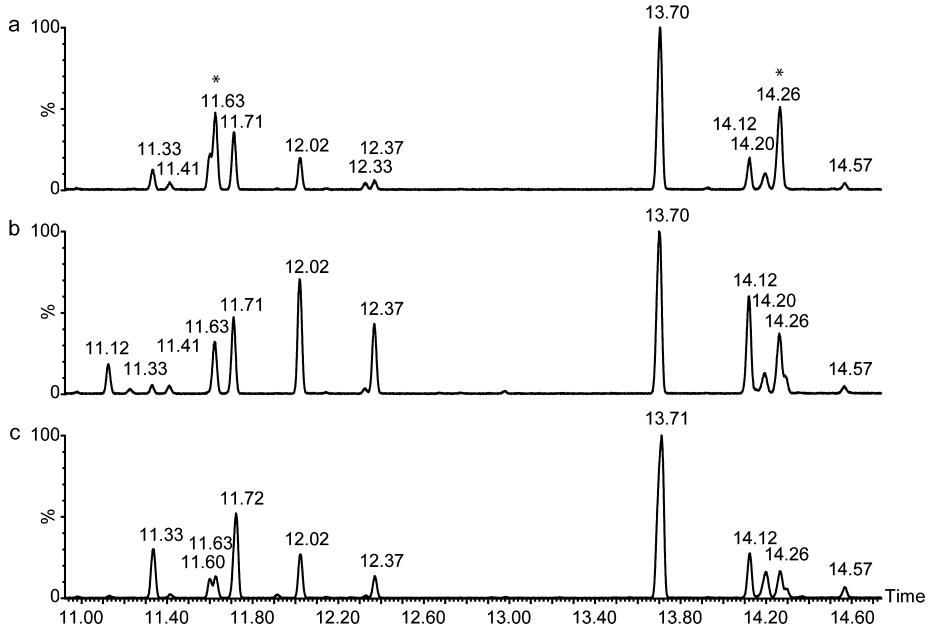

Figure 1. Representative GC-MS total ion chromatograms for the M202 variety: (a) control (day 0), (b) 3 days of submergence, and (c) 3 days of submergence + 1 day of postsubmergence recovery. Identified metabolites include Asp (14.12 min), GABA (14.28 min), glycerate (11.60 min), Gly(11.33 min), Ile (11.12 min), malate (13.71 min), pyroglutamate (14.20 min), Ser (12.02 min), succinate (11.41 min), Thr (12.37 min), and threonate (14.57 min). Peaks due to FAMES markers are indicated with an asterisk at 11.63 and 14.26 min.

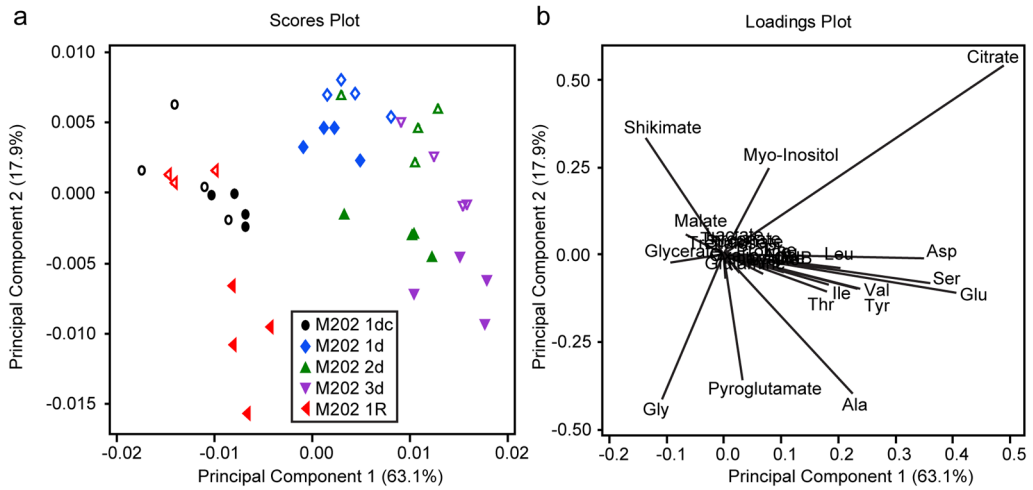

Figure 2. Scores plot (a) showing principal components 1 and 2. The legend identifies the individual treatments for the M202 variety. The same scheme but with open symbols was used to represent the M202(*Sub1*) samples. The loadings plot (b) shows the variables that contributed most to the variance along the first and second principal components.

data were deisotoped. The results were exported to Excel (Microsoft, Redmond, WA) where the retention times and the extracted masses were matched with identified metabolites. One mass−retention time pair with the corresponding area for each metabolite was taken for data normalization and statistical analysis. The mass−retention time pair with the highest relative abundance was chosen to represent each metabolite (excluding the silylation-related fragments 73 and 147 m/z).

Statistical Analyses

The data were normalized by dividing the area of the individual components by the summed area for all the identified metabolites as described by Lee et al.[6] P values were calculated in Excel using a two-tailed Student's t test comparing inter- and intragenotype differences as a result of submergence stress or recovery. The GC-MS results for one member of the M202(*Sub1*) 1 day of recovery (1R) sample set were excluded from the statistical analysis due to poor sensitivity and the presence of peaks inconsistent with the rest of the data set. Trajectory plots were prepared with Origin 7.5 (OriginLab, Northampton, MA) using the average and standard deviations determined for each treatment. The integrated, sum-normalized areas of mass−retention time pairs from the identified metabolites was used for principal components analysis (PCA) carried out with Minitab 15 (Minitab, Inc., State Park, PA) after mean-centering in Excel.

RESULTS AND DISCUSSION

This study examines the differences in the GC-MS metabolite profiles measured for extracts of M202 and M202(*Sub1*)

dx.doi.org/10.1021/pr300953k | J. Proteome Res. 2013, 12, 898−909

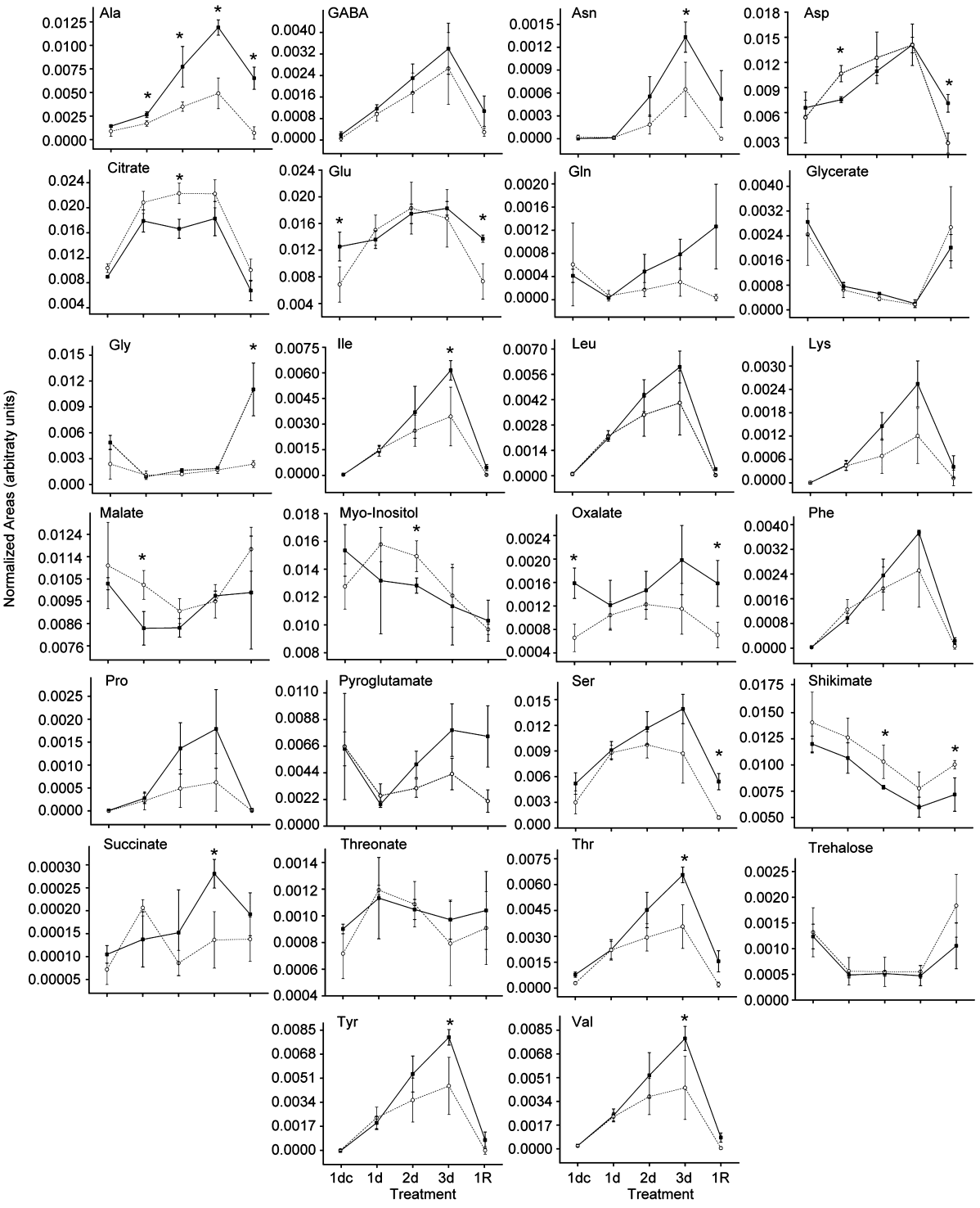

Figure 3. Trajectory plots from the GC-MS experiments representing the average normalized relative peak areas for M202 (■) and M202(*Sub1*) (○). Time points are connected using solid (M202) or dotted [M202(*Sub1*)] lines. Treatments are labeled as 1 day of control (1dc), 1, 2, and 3 days of submergence (1d, 2d, and 3d), and 3 days of submergence + 1 day of postsubmergence recovery (1R). Each data point represents the average of at least three biological replicates with error bars representing the standard deviation and asterisks indicating differences between the genotypes with a P value <0.05.

seedlings subjected to control, submergence stress, and recovery conditions. These GC-MS results are then compared to our previously published analysis of the metabolic response for these genotypes measured using ^{1}H NMR.[24] In both sets of experiments, aliquots of the same tissue samples were extracted and analyzed.

Figure 1 shows a region of the representative total ion chromatograms (TICs) measured for M202 rice extracts comparing the results obtained for control, 3 days of submergence, and 1 day of postsubmergence recovery samples. Several organic and amino acids are detected in this region of the TIC including aspartate (Asp), γ-aminobutyric acid (GABA),

dx.doi.org/10.1021/pr300953k | J. Proteome Res. 2013, 12, 898−909

Table 1. Comparison of the Treatment and Control Levels of Metabolites as Represented by Fold Changes for M202 and M202(*Sub1*) Relative to the Controls and between the Two Varieties for Each Treatment Condition[a]

		M202				M202(*Sub1*)				M202/M202(*Sub1*)				
class	metabolites	1d:1dc	2d:1dc	3d:1dc	1R:1dc	1d:1dc	2d:1dc	3d:1dc	1R:1dc	1dc	1d	2d	3d	1R
sugars	trehalose	0.4*	ND	ND	0.9	0.4	ND	ND	0.8	0.9	ND	ND	ND	0.6
amino acids	Ala	2.1*	7.0*	8.7*	4.7*	1.9	3.3*	5.2	0.8	1.4	1.5*	3.0*	2.3*	8.3*
	Asn	ND	ND	ND	ND	ND	ND	ND	ND	ND	0.8	3.5	2.8*	ND
	Asp	1.1	1.7*	2.1*	1.1	2.0	2.3*	2.6*	0.4	1.2	0.7*	0.9	1.0	3.0*
	Gln	ND	ND	ND	ND	ND	ND	ND	ND	ND	ND	ND	ND	ND
	Glu	1.0	1.4*	1.5*	1.1	2.2*	2.7*	2.6*	1.1	1.8*	0.9	1.0	1.0	1.9*
	Gly	0.2*	0.4*	0.4*	2.5*	0.5	0.5	0.7	1.0	1.8	0.8	1.4	1.1	4.6*
	Ile	ND	ND	ND	ND	ND	ND	ND	ND	ND	0.9	1.7	1.8*	ND
	Leu	ND	ND	ND	ND	ND	ND	ND	ND	ND	0.9	1.3	1.5	ND
	Lys	ND	ND	ND	ND	ND	ND	ND	ND	ND	0.9	2.3	1.9	3.3
	Phe	ND	ND	ND	ND	ND	ND	ND	ND	ND	0.7	1.3	1.4	ND
	Pro	ND	ND	ND	ND	ND	ND	ND	ND	ND	ND	ND	ND	ND
	pyroglutamate	0.3*	0.8	1.2	1.2	0.4	0.5	0.7	0.3	1.0	0.7	1.6	1.8*	3.6*
	Ser	1.7*	2.4*	2.7*	1.0	2.9*	3.2*	3.1*	0.4	1.7	1.0	1.3	1.5	4.4*
	Thr	ND	ND	ND	ND	ND	ND	ND	ND	ND	0.9	1.7	1.8*	ND
	Tyr	ND	ND	ND	ND	ND	ND	ND	ND	ND	0.8	1.6	1.6*	ND
	Val	ND	ND	ND	ND	ND	ND	ND	ND	ND	1.0	1.6	1.8*	ND
organic acids	citrate	2.0*	1.9*	2.0*	0.8	2.0*	2.2*	2.2*	1.0	0.9	0.9	0.8*	0.8	0.7
	glycerate	0.3*	0.2*	0.1*	0.7*	0.3	0.1	0.1	1.1	1.2	1.2	1.5	1.3	0.8
	GABA	ND	ND	ND	ND	ND	ND	ND	ND	ND	1.1	1.3	1.1	ND
	malate	0.8*	0.8*	0.9	0.9	0.9	0.8	0.9	1.1	0.9	0.8*	1.0	1.0	0.8
	oxalate	0.6*	1.0	1.2	1.0	1.6	1.9*	1.4	1.1	2.4*	1.0	1.3	2.2	2.2*
	shikimate	0.9	0.7*	0.5*	0.6*	0.9	0.7	0.6	0.7	0.9	0.9	0.8*	0.7	0.7*
	succinate	1.2	1.9*	2.7*	1.8*	2.9*	1.2	1.6	1.9	1.5	0.6	2.3	2.4*	1.4
	threonate	1.4	1.1*	1.1	1.2	1.7*	1.5	1.3	1.3	1.3	1.1	0.9	1.0	1.1
other metabolites	myo-inositol	0.8	0.9	0.7*	0.7*	1.2	1.2	1.0	0.8	1.2	0.8	0.9*	0.9	1.1

[a]Asterisks represent significant differences at the 95% confidence limit. ND represents metabolite ratios that are not determined due to values below the limit of quantitation.

glycerate, glycine (Gly), isoleucine (Ile), malate, pyroglutamate, serine (Ser), succinate, Thr, and threonate. Differences in relative metabolite abundance as a consequence of treatment are evident by visual inspection of Figure 1, with some peaks increasing in intensity, others decreasing, and some appearing to remain unchanged.

Metabolomics Analyses of the Stress Response

Global analysis of the metabolic changes due to submergence and recovery stresses was performed by PCA (Figure 2). PC1 and PC2 represent 63.1 and 17.9%, respectively, of the explained variance with distinct groupings observed for the two varieties during stress conditions. In the absence of stress, the control treatments do not separate based on genotype in the PCA scores plot (Figure 2a). Within 1 day of submergence stress, both genotypes cluster to the right of the controls along PC1, whereas the tolerant and intolerant varieties differ along the second component. The distinction between M202 and M202(*Sub1*) in Figure 2a remains consistent over the course of the treatment, with the sample trajectory moving further along PC1 with duration of submergence and with the two varieties maintaining their separation in PC2. The data for the tissue samples after 1 day of recovery shift back toward the controls. The 1 day recovery samples of the submergence-tolerant M202(*Sub1*) variety cluster with the controls, while the intolerant M202 samples are clustered below, well-separated from the controls in PC2.

Overall, the GC-MS PCA results in Figure 2 are consistent with the previously reported PCA analysis of the ^{1}H NMR data;[24] however, there are fundamental differences between the two data sets that can be attributed to several factors. PCA of the NMR data used over 300 variables generated by integrating "bins" of the NMR spectrum in equidistant sections allowing use of the entire spectrum, with the exception of solvent peaks. As a result, more NMR variables were available to define the differences between the data sets. PCA of the GC-MS results was conducted only with the identified variables because unidentified peaks can result from side reactions characteristic of the derivatization process. The advantage of including only the identified metabolites in the PCA analysis can be seen in Figure 2b. The variables representing the largest separation along PC1, PC2, or in both dimensions (e.g., citrate and shikimate) are clearly identified as important in the loadings plot. Metabolites that contribute to separation primarily along PC1 are Asp, glutamate (Glu), Ile, Ser, Thr, and tyrosine (Tyr). Contributions to PC2 can be attributed to Ala, Gly, myo-inositol, and pyroglutamate. Despite the distinct grouping of the two varieties in Figure 2a, PCA is unable to define statistical differences or quantitative relationships between the varieties during stress. This level of information requires a direct comparison of the

dx.doi.org/10.1021/pr300953k | J. Proteome Res. 2013, 12, 898−909

results obtained for each metabolite in samples measured at the different stress time points.

Metabolite Profiles Determined by GC-MS

The differences between metabolite levels in the two genotypes were examined to better understand the metabolic shifts resulting from submergence and recovery. Metabolite profiles for the control, submergence, and recovery treatments were measured using GC-MS for 17 amino acids, seven organic acids, myo-inositol, and trehalose and are summarized in the trajectory plots shown in Figure 3. These differences are also apparent in Table 1, which examines the fold changes of individual metabolites over time within and between genotypes.

Similar to what was previously reported by ^{1}H NMR,[24] the GC-MS analysis presented in Figure 3 shows that 15 of the 17 detected amino acids also accumulated during submergence and showed a return toward pretreatment values after 24 h of recovery. Significant differences (P value ≤ 0.05) between the genotypes were evident in the levels of 11 of the 17 detected amino acids either at some time point of the submergence treatment or after 24 h of recovery (Table 1). Amino acid metabolism reflects a stress response involving pathways related to elevated carbon catabolism through glycolysis and nitrogen utilization. Amino acids accumulated in both varieties during submergence stress; however, this trend was more prominent for the intolerant variety, supporting the previous observation that M202 has higher levels of starch consumption and sugar catabolism to generate ATP to fuel underwater elongation growth.

In contrast to the behavior of the majority of the amino acids, Gly levels in the intolerant variety increased 2.5-fold above nonstressed levels during recovery after reoxygenation (Figure 3 and Table 1). Gly is directly related to the metabolism of several amino acids, including Ser and Thr, and the increase in Gly levels could result from the recycling of these amino acids.[30] However, the tolerant variety also accumulates Ser and Thr during submergence, although at lower amounts, and does not show a corresponding increase in Gly after 24 h of recovery. The stasis of Gly in samples of M202(*Sub1*) for all treatment conditions examined supports the assertion that increases in Gly levels in M202 may be a mechanistic response to reoxygenation/dehydration stress. Because reoxygenation and dehydration stresses are affected by the presence of *SUB1*A and *SUB1*A-containing varieties are more tolerant to dehydration, the observation in Figure 3 that Gly does not increase during recovery in the tolerant cultivar could be associated with the better reoxygenation tolerance of this genotype. This is consistent with reports of Gly accumulation in other plants as a result of increased photorespiration during dehydration.[31] There may be other reasons for this distinction in Gly accumulation during submergence recovery. A recent report suggests that Gly can act as a ligand for ligand-mediated gating of calcium in plants.[32] Calcium signaling is important for a variety of plant stress responses, including synergistic control of stomata opening with abscisic acid[33] and increased production of alcohol dehydrogenase, a key enzyme in anaerobic metabolism, during oxygen deprivation.[34,35] Alternatively, Gly accumulation observed in the M202 samples may not be a result of the catabolism of pathway-related metabolites but instead a response to reoxygenation or dehydration stresses experienced by plants after prolonged submergence.[23]

Pyroglutamate is an uncommon amino acid related to glutathione metabolism and also commonly found at the N termini of proteins.[36,37] In both rice varieties, pyroglutamate levels decrease during the first day of submergence (Figure 3). Over the subsequent 2 days, levels of pyroglutamate in M202 return to prestress levels, while in M202(*Sub1*) they remain lower than the controls for the duration of the study, including the recovery period. This divergence in pyroglutamate levels for the two varieties could be indicative of differences in glutathione metabolism or protein turnover.

Energy production is a key component of plant survival, especially under submergence conditions where photosynthesis can be dramatically reduced as a result of limited diffusion of carbon dioxide.[38] As a result of submergence stress, significant differences between the two genotypes were observed in the levels of the detected TCA cycle intermediates and components of related pathways (Figure 3). For the intolerant variety, citrate, GABA, and succinate increased in abundance throughout the course of submergence and then decreased after reoxygenation. Interestingly, citrate and succinate exhibited differing trends over the 3 day submergence treatment. After an initial accumulation within the first day of submergence, citrate plateaued and subsequently decreased upon reoxygenation. Succinate gradually accumulated, with an apex at day 3 of submergence before decreasing during reoxygenation. In contrast, malate decreased during the first day of submergence, while the reoxygenation time point is inconclusive due to high variance. The sudden accumulation and plateau of citrate without detecting a corresponding increase in isocitrate or α-ketoglutarate suggest that either the TCA cycle is regulated at citrate or that the flux through the subsequent intermediates is fast. The gradual increase of succinate, however, suggests a noncircular pathway for the TCA cycle through 2-oxoglutarate or oxaloacetate. Both are produced in the metabolism of pyruvate and glutamate to Ala. GABA, which also gradually accumulates during stress, is generated from 2-oxyoglutarate and has been reported to be produced during anaerobic metabolism.[39] GABA is also part of the photorespiration pathway, producing succinic semialdehyde, Gly, and Ala, corroborating the accumulation of Gly in the intolerant variety.[40] The lack of change in Gly for the tolerant variety is still puzzling. The production of Gly requires glyoxylate, which was not monitored in this study. Monitoring glyoxylate production in the two rice varieties as well as flux studies could provide a better understanding of this difference between the two rice varieties in Gly production. Interestingly, succinate accumulation trends follow a similar trajectory as Ala and the other detected TCA cycle intermediates (Figure 3). In addition, the reduction of malate levels during submergence suggests a slowing of the TCA cycle, supporting the regulation of the TCA cycle at citrate and the accumulation of succinate through alternative pathways. Malate could also be converted to pyruvate, possibly providing additional means of carbon storage during oxygen stress; however, flux analysis is necessary to fully understand the role of the detected TCA cycle intermediates.[41] The results obtained for the TCA intermediates argue for future flux experiments. Because these experiments are complex and require expensive stable isotope-labeled compounds, advance knowledge of the pathways of interest is critical.

Although the trends for citrate and GABA in the tolerant variety are similar to those observed for M202, the disparity between the genotypes is evident in the time-course plots for these TCA-related metabolites (Figure 3). Succinate increased drastically in M202(*Sub1*) samples after the first day of submergence, decreased back to initial levels after 2 days, and then remained unchanged. The accumulation of succinate in

dx.doi.org/10.1021/pr300953k | J. Proteome Res. 2013, 12, 898−909

M202 was 2.4 times that of M202(*Sub1*) by 3 days (Table 1); however, no statistically significant differences between the varieties were observed at the other points examined. Citrate and malate differed from other metabolites in that levels in M202(*Sub1*) were higher than those measured for the intolerant variety. The first day of submergence resulted in 0.8 times less malate for the intolerant variety as compared to the tolerant variety. Similarly, citrate was 0.8 times less abundant in M202 as compared to levels in the M202(*Sub1*) samples (Table 1). Although these were the only time points where statistically significant differences (P value ≤ 0.05) between the two varieties were observed, this general trend is consistent throughout the course of the experiment. The higher levels of the TCA cycle intermediates detected in the tolerant variety could reflect the greater photosynthetic capacity of M202(*Sub1*) due to the presence of more chlorophyll during submergence as reported by Fukao et al.[19,23]

Despite the sensitivity of GC-MS measurements, we were unable to quantify the sugars sucrose, glucose, and fructose due to the method selected and the nature of the TOF instrument available for this work. Sucrose is the primary metabolite in rice extracts, dominating the other metabolites by a significant margin. NMR is able to accommodate a $\sim 10^6$ dynamic range as compared to 10^4 for the Waters GCT Premier when using dynamic range enhancement feature, which was not employed in this study.[16,42] To observe the less abundant compounds and take full advantage of the sensitivity of our GCT Premier TOF instrument, we did not attempt to quantify these soluble sugars (glucose, sucrose, and fructose) because of detector overload at the concentrations necessary to adequately quantify other metabolites. Also, because sucrose and glucose were easily quantified using ^{1}H NMR, there was not a strong motivation to attempt to measure these analytes by GC-MS. However, glycerate, a sugar alcohol, and trehalose were detected by GC-MS and observed to decrease during submergence in both genotypes. During submergence, trehalose levels drop below the limit of quantification, preventing a metabolic comparison of the genotypes. The metabolite profiles for glycerate in M202 and M202(*Sub1*) are indistinguishable, suggesting that the levels of this compound are not impacted by the presence of *SUB1*A.

Narsai et al. explored the anaerobic germination of *O. sativa* cv. Amaroo (also a *japonica* subspecies) using a variety of "-omics" techniques, including metabolite profiling by GC-MS.[29] They reported changes in 166 metabolites during the course of their experiment, which is significantly more than the 30 metabolites reported in this study in both the NMR and the GC-MS data sets (Table 2). There are several possibilities that might explain the different numbers of metabolites observed in these two studies. The plant growth stage at the time of harvest greatly influences the numbers of detected metabolites.[43] The anoxia study performed by Narsai et al. examined embryos grown in the dark in either anaerobic or aerobic conditions and separated from the endosperm within a few days of germination.[29] The study reported herein used seedlings sampled within 17 days of germination (12 days after planting) and grown under aerobic conditions until submergence stressed. Several reports have indicated that metabolic content varies during plant and fruit development, especially during the germination and development of young plants.[43−46] The experiments of Narsai et al. were also performed using a different rice variety than used in this study.[29] Using GC-MS and ^{1}H NMR, we have shown significant metabolic differences as a result of submergence stress for two varieties differing in the presence or absence of a single gene, *SUB1A*.[24] Differences between cultivars can be much more significant, resulting in a wider range of metabolites produced in response to anaerobic stress. Finally, the greater number of metabolites reported by Narsai et al. could be attributed in part to the quadrupole mass analyzer used in their study, which has a wider linear quantitation range than our TOF instrument.[47] However, despite the greater number of metabolites detected in their study, neither SMM nor AlaGly, which we detected using ^{1}H NMR, were reported by Narsai and co-workers.

Table 2. Metabolites Quantified by GC-MS and NMR[a]

class	metabolites	NMR	GC-MS
sugars	glucose	×	
	sucrose	×	
	trehalose		×
amino acids	Ala	×	×
	Asn	×	
	Asp	×	×
	Gln	×	×
	Glu	×	×
	Gly		×
	Ile	×	×
	Leu	×	×
	Lys		×
	Phe		×
	Pro		×
	pyroglutamate		×
	Ser	×	×
	SMM	×	
	Thr	×	×
	Tyr	×	×
	Val	×	×
organic acids	citrate		×
	glycerate		×
	GABA		×
	malate		×
	oxalate		×
	shikimate	×	×
	succinate		×
	threonate		×
other metabolites	AlaGly	×	
	myo-inositol		×

[a]The "×" denotes detection of the metabolite by either NMR, GC-MS, or both instruments.

Comparison of the GC-MS and NMR Results

Because of the fundamental differences in the nature of GC-MS and NMR measurements, the results obtained using each platform contributed to our understanding of the complex metabolic response of rice to submergence stress. Table 2 lists the metabolites quantified in this study and the instrument used for their measurement. In total, four metabolites, sucrose, glucose, AlaGly, and SMM, were exclusively quantified by NMR.[24] Fourteen metabolites including several organic acids, TCA cycle intermediates, and amino acids were exclusively quantified by GC-MS, and 11 metabolites were determined by both instruments. Increased signal averaging could have been used to improve the sensitivity of NMR quantitation of the less abundant metabolites; however, this approach rapidly becomes impractical because improvement in S/N is proportional to the

dx.doi.org/10.1021/pr300953k | J. Proteome Res. 2013, 12, 898−909

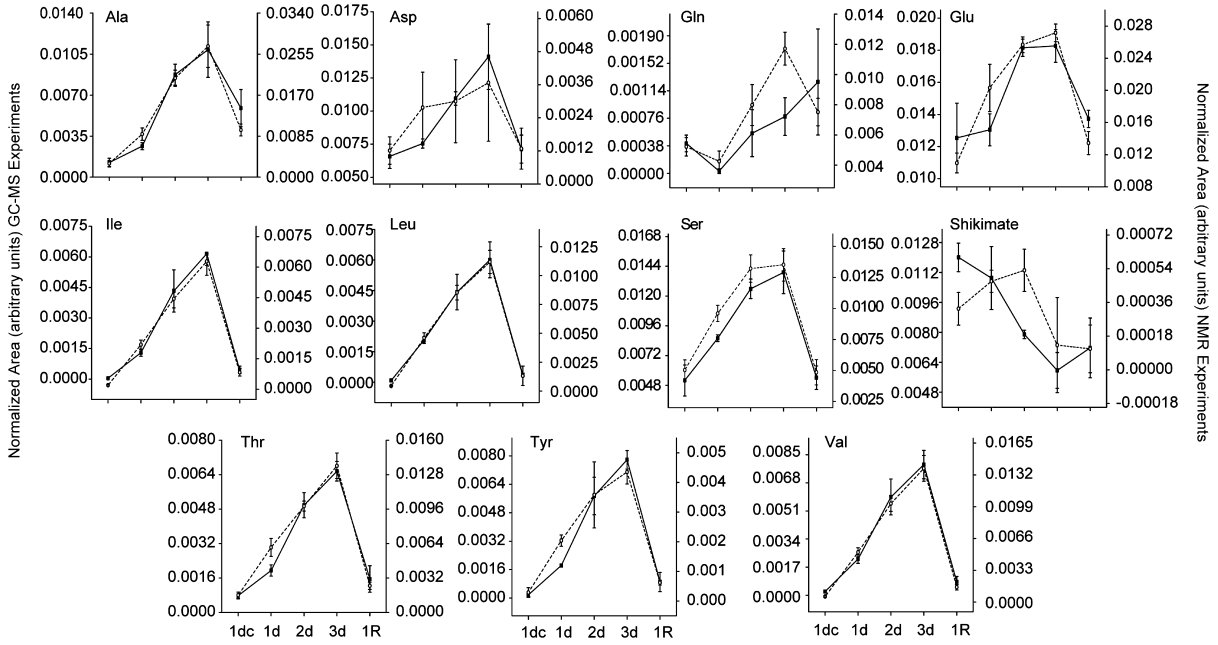

Figure 4. Trajectory plots comparing the normalized metabolic profiles measured using ^{1}H NMR (○) and GC-MS (■). Time points indicate controls (1dc), 1, 2, and 3 days of submergence (1d, 2d, and 3d), or 3 days of submergence followed by 1 day of postsubmergence recovery (1R). Each data point represents the averaged normalized area of at least three biological replicates for the GC-MS data or five biological replicates for the NMR data with error bars indicating the standard deviation.

square root of the number of coadded transients.[16,48] Furthermore, several compounds that were detected by GC-MS were not observed in the NMR spectrum due to problems of resonance overlap, for example, the Gly resonance, which is obscured by the more intense sucrose resonances.

The analytical and biological reproducibility of the GC-MS and ^{1}H NMR results can be evaluated by comparing the metabolite trajectories obtained for overlapping metabolites quantified for M202 using both instruments. Overlaid in Figure 4 are trajectory plots from both NMR and GC-MS experiments for different extracts of the same tissue samples from the M202 tissue. Figure S1 in the Supporting Information shows a similar set of plots for M202(*Sub1*). Peak areas determined in both experiments are normalized, with the GC-MS data normalized to all identified metabolites (as described in section 2.8) and the NMR data sum normalized as described in Barding et al.[24] A strong correlation between the two data sets is observed in both Figure 4 and Figure S1 in the Supporting Information, with the profiles for most metabolites displaying similar trends throughout the course of treatment. The profiles for Gln and shikimate show the greatest degree of difference between the data sets. From the GC-MS data set, shikimate decreases during the course of submergence, whereas a decrease was not apparent in the NMR data until the 3 day time point. Although the trends are similar for both data sets, the relative abundance of shikimate in the NMR data set is low, and the resonances for shikimate appear in a crowded region of the spectrum, complicating the deconvolution process. In contrast, shikimate is easily detected and quantified by GC-MS, making the measurements more reliable for qualitative and quantitative analysis. The opposite was true for Gln, where it was readily quantified by NMR but detected in relatively low abundance by GC-MS analysis.

Some differences between the data sets shown in Figures 4 and S1 in the Supporting Information can be attributed to the higher standard deviation of the GC-MS data set for those time points and to differences in data normalization. Although data from both techniques were sum normalized, GC-MS data were normalized to the sum total of all identified components, whereas for the NMR results, the integrated areas of both identified and unidentified components were used. Despite the minor differences observed in Figures 4 and S1 in the Supporting Information, these results show how data sets collected by two very different analytical methods can also provide confidence in the validity of data preprocessing.

For some analytes, such as Gln (Figure S2 in the Supporting Information), differences in the NMR and GC-MS results can be attributed to differences in S/N. For both data sets, the Glu peak is present at higher intensity than Gln; however, the Gln peak is of much lower relative intensity in the GC-MS data set, and Gln was not detected in the 1 and 2 day samples. In contrast, the Gln resonances are readily detected in the NMR spectra for all time points evaluated. To better understand the differences between the data sets, S/N was measured for the Glu and Gln peaks for each data set (Table S1 in the Supporting Information). At time points where Gln was detected by GC-MS, the S/N was ∼5% that of Glu. When measured by NMR, the S/N of Gln was between 20 and 70% that of Glu, and Gln was always present at quantifiable levels. Because Gln and Glu are important in plant nitrogen metabolism,[49] understanding the relationship between the two amino acids is important.

Detection of AlaGly and SMM

Previously, we reported the identification of the dipeptide AlaGly in rice extracts by ^{1}H NMR analysis.[24] Interestingly, AlaGly was not reported in recent GC-MS-based rice metabolite profiling studies, nor is it included in publicly available metabolomics libraries.[13,14,29] A cursory analysis of the GC-MS results of our rice extracts also failed to identify AlaGly, which contrasted with the pronounced intensity of AlaGly resonances in the ^{1}H NMR spectra measured for the same tissue samples. Figure 5 shows a representative ^{1}H NMR spectrum and GC-MS total ion chromatogram (TIC). Because of the inherently quantitative

dx.doi.org/10.1021/pr300953k | J. Proteome Res. 2013, 12, 898−909

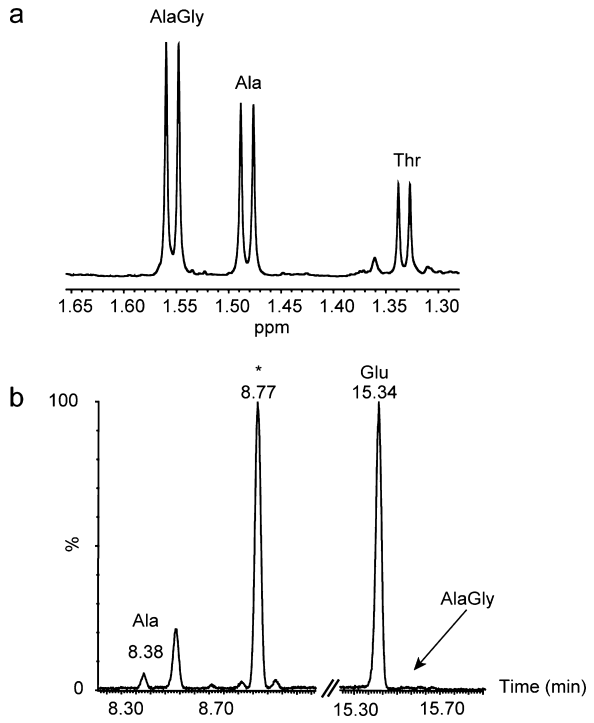

Figure 5. ^{1}H NMR spectrum (a) and GC-MS chromatogram (b) measured for extracts of the same M202 control rice tissue showing the differences in the response of the two analytical platforms for Ala and AlaGly. AlaGly is present in greater abundance than Ala in this sample as judged by the relative intensity of the NMR resonances but is not detectable in the GC-MS TIC. The retention time indicated on the chromatogram in panel b shows the expected elution time based injection of an AlaGly standard. An asterisk indicates the FAMEs retention index marker in panel b.

nature of NMR, comparison of the relative integrals of the methyl resonances for AlaGly (1.66) and Ala (1.00) in Figure 5a provides a direct quantitative relationship of the relative concentrations of the two compounds in the extract. Although GC-MS is generally considered to have greater sensitivity than NMR, AlaGly is not detected by GC-MS in Figure 5b. Because AlaGly could not be identified by deconvolution and library matching, a standard was derivatized and injected to establish the expected GC elution time for comparison with the rice tissue extracts. Several factors could be responsible for much lower detection sensitivity for AlaGly including low volatility, hydrogen bonding to the injector liner, or poor derivatization efficiency.

SMM is another metabolite that we readily detected by ^{1}H NMR but did not observe by GC-MS analysis of rice extracts. SMM can play an important role in ethylene production as well as sulfur transport and has been previously shown to accumulate in anoxic rice seedlings.[25,26,28] Although NMR analysis of the submergence treated tissue did not reveal significant changes in the levels of SMM in the two genotypes, its absence from the GC-MS data was enigmatic. The positive formal charge of SMM could reduce its volatility and increase its ability to bond with various parts of the inlet and column. Another factor in its low sensitivity could be excessive fragmentation by the electron ionization (EI) source. Comparison of the mass spectra of AlaGly, Ala, and SMM (Figure S2 in the Supporting Information) reveals that AlaGly and Ala both produce the same major fragment ions (m/z 73, 75, and 116) with differences between the molecules observable in the very low abundance ions. In contrast, SMM is heavily fragmented, producing many ions at relatively high abundance with the m/z 176 ion as the most intense peak.

CONCLUSIONS

The goal of untargeted metabolomics experiments is to sample as much of the metabolite chemical space as possible. As this study has shown, this is best accomplished using multiple analytical platforms. The GC-MS results both corroborated and complemented our previous NMR study. Metabolites exclusively detected by GC-MS analysis include the amino acids Phe, Pro, pyroglutamate, the TCA intermediates citrate, malate, and succinate, as well as the organic acids GABA, glycerate, oxalate, shikimate, and threonate. These metabolites provided additional support for carbohydrate regulation by *SUB1*A during submergence as evident through pyruvate metabolism to Ala and changes in the levels of GABA, TCA cycle intermediates, and other amino acids. Possible points of regulation of the TCA cycle and evidence for alternative, noncyclic pathways were revealed by GC-MS through the rapid elevation of citric acid and gradual accumulation of GABA and succinate. A possible biomarker for dehydration or reoxygenation stress was also evident in the intolerant variety through accumulation of Gly, which may affect cellular signaling pathways during the recovery period. The increase in relative abundance of pyroglutamate may also be an indicator of oxidative stress during and after submergence due to its role in glutathione metabolism.

Throughputs of both platforms were comparable in terms of the time required for measurements and data processing, while the advantages and disadvantages of each platform were complementary. NMR is inherently quantitative, universally detects organic compounds, and has a high dynamic range. However, NMR is generally considered to be less sensitive than GC-MS, and in the analysis of whole plant extracts, it can be difficult to resolve signals for some compounds due to resonance overlap. Although GC-MS was able to detect 14 compounds not observed by NMR, three important metabolites, Gln, AlaGly, and SMM, were more readily detected and quantified by ^{1}H NMR. The dynamic range limitations of the TOF mass analyzer available for this work reduced somewhat the utility of GC-MS; however, the dynamic range of the measurements could be effectively expanded by using split injections or performing measurements of extracts at differing degrees of dilution. Taken together, these results demonstrate that the complementary use of ^{1}H NMR and GC-MS can facilitate a more thorough exploration of the metabolome of the biological system in question.

ASSOCIATED CONTENT

Supporting Information

Additional figures and tables. This material is available free of charge via the Internet at http://pubs.acs.org.

AUTHOR INFORMATION

Corresponding Author

*Tel: 951-827-2990. Fax: 951-827-4713. E-mail: clarive@ucr.edu.

Notes

The authors declare no competing financial interest.

■ ACKNOWLEDGMENTS

This work was supported by the National Science Foundation (Grant No. IOS−1121626) and the U.S. Department of Agriculture, National Institute of Food and Agriculture - Agriculture and Food Research Initiative (Grant No. 2011−04015) to C.K.L, J.B.-S., and T.F., and a National Science Foundation Integrative Graduate Education Research and Training Program fellowship (DGE-0504249) to G.A.B. S.B. acknowledges support from KTIA-OTKA MB08A/80066.

■ REFERENCES

(1) Liu, G.; Wang, Y.; Wang, Z.; Cai, J.; Lv, X.; Zhou, A. Metabolomic studies on the biochemical profile of urine from rats with acute cysteamine supplementation. *Metabolomics* **2011**, *7* (4), 536−541.

(2) Ruan, C.-J.; da Silva, J. A. T. Metabolomics: Creating new potentials for unraveling the mechanisms in response to salt and drought stress and for the biotechnological improvement of xero-halophytes. *Crit. Rev. Biotechnol.* **2011**, *31* (2), 153−169.

(3) Kim, J. D.; Kaiser, K.; Larive, C. K.; Borkovich, K. A. Use of H-1 nuclear magnetic resonance to measure intracellular metabolite levels during growth and asexual sporulation in *Neurospora crassa*. *Eukaryotic Cell* **2011**, *10* (6), 820−831.

(4) Reaves, M. L.; Rabinowitz, J. D. Metabolomics in systems microbiology. *Curr. Opin. Biotechnol.* **2011**, *22* (1), 17−25.

(5) Flores-Valverde, A. M.; Horwood, J.; Hill, E. M. Disruption of the steroid metabolome in fish caused by exposure to the environmental estrogen 17 alpha-ethinylestradiol. *Environ. Sci. Technol.* **2010**, *44* (9), 3552−3558.

(6) Lee, D. Y.; Fiehn, O. High quality metabolomic data for *Chlamydomonas reinhardtii*. *Plant Methods* **2008**, *4*, 13.

(7) Ramautar, R.; Busnel, J. M.; Deelder, A. M.; Mayboroda, O. A. Enhancing the coverage of the urinary metabolome by sheathless capillary electrophoresis-mass spectrometry. *Anal. Chem.* **2012**, *84* (2), 885−892.

(8) Wikoff, W. R.; Gangoiti, J. A.; Barshop, B. A.; Siuzdak, G. Metabolomics identifies perturbations in human disorders of propionate metabolism. *Clin. Chem.* **2007**, *53* (12), 2169−2176.

(9) Fiehn, O.; Kopka, J.; Trethewey, R.; Willmitzer, L. Identification of uncommon plant metabolites based on calculation of elemental compositions using gas chromatography and quadruple mass spectrometry. *Anal. Chem.* **2000**, *72* (15), 3573−3580.

(10) Brown, F. F.; Campbell, I. D.; Kuchel, P. W.; Rabenstein, D. C. Human erythrocyte metabolism studies by H-1 spin-echo NMR. *FEBS Lett.* **1977**, *82* (1), 12−16.

(11) Gavaghan, C. L.; Li, J. V.; Hadfield, S. T.; Hole, S.; Nicholson, J. K.; Wilson, I. D.; Howe, P. W. A.; Stanley, P. D.; Holmes, E. Application of NMR-based metabolomics to the investigation of salt stress in maize (Zea mays). *Phytochem. Anal.* **2011**, *22* (3), 214−224.

(12) Strehmel, N.; Hummel, J.; Erban, A.; Strassburg, K.; Kopka, J. Retention index thresholds for compound matching in GC-MS metabolite profiling. *J. Chromatogr., B* **2008**, *871*, 182−190.

(13) Wishart, D. S.; Knox, C.; Guo, A. C.; Eisner, R.; Young, N.; Gautam, B.; Hau, D. D.; Psychogios, N.; Dong, E.; Bouatra, S.; Mandal, R.; Sinelnikov, I.; Xia, J.; Jia, L.; Cruz, J. A.; Lim, E.; Sobsey, C. A.; Shrivastava, S.; Huang, P.; Liu, P.; Fang, L.; Peng, J.; Fradette, R.; Cheng, D.; Tzur, D.; Clements, M.; Lewis, A.; De Souza, A.; Zuniga, A.; Dawe, M.; Xiong, Y.; Clive, D.; Greiner, R.; Nazyrova, A.; Shaykhutdinov, R.; Li, L.; Vogel, H. J.; Forsythe, I. HMDB: A knowledgebase for the human metabolome. *Nucleic Acids Res.* **2009**, *37*, D603−D610.

(14) Kopka, J.; Schauer, N.; Krueger, S.; Birkemeyer, C.; Usadel, B.; Bergmuller, E.; Dormann, P.; Weckwerth, W.; Gibon, Y.; Stitt, M.; Willmitzer, L.; Fernie, A. R.; Steinhauser, D. GMD@CSB.DB: The Golm Metabolome Database. *Bioinformatics* **2005**, *21* (8), 1635−1638.

(15) Holzgrabe, U.; Diehl, B. W. K.; Wawer, I. NMR spectroscopy in pharmacy. *J. Pharm. Biomed. Anal.* **1998**, *17* (4−5), 557−616.

(16) Jacobsen, N. E. *NMR Spectroscopy Explained: Simplified Theory, Application, and Examples for Organic Chemistry and Structural Biology*; John Wiley and Sons, Inc.: Hoboken, 2007.

(17) Beckonert, O.; Keun, H. C.; Ebbels, T. M. D.; Bundy, J. G.; Holmes, E.; Lindon, J. C.; Nicholson, J. K. Metabolic profiling, metabolomic and metabonomic procedures for NMR spectroscopy of urine, plasma, serum and tissue extracts. *Nat. Protoc.* **2007**, *2* (11), 2692−2703.

(18) Cui, Q.; Lewis, I. A.; Hegeman, A. D.; Anderson, M. E.; Li, J.; Schulte, C. F.; Westler, W. M.; Eghbalnia, H. R.; Sussman, M. R.; Markley, J. L. Metabolite identification via the Madison Metabolomics Consortium Database. *Nat. Biotechnol.* **2008**, *26* (2), 162−164.

(19) Fukao, T.; Xu, K. N.; Ronald, P. C.; Bailey-Serres, J. A variable cluster of ethylene response factor-like genes regulates metabolic and developmental acclimation responses to submergence in rice(W). *Plant Cell* **2006**, *18* (8), 2021−2034.

(20) Voesenek, L.; Bailey-Serres, J. Plant Biology: Genetics of high-rise rice. *Nature* **2009**, *460* (7258), 959−960.

(21) Xu, K.; Xu, X.; Fukao, T.; Canlas, P.; Maghirang-Rodriguez, R.; Heuer, S.; Ismail, A. M.; Bailey-Serres, J.; Ronald, P. C.; Mackill, D. J. SUB1A is an ethylene-response-factor-like gene that confers submergence tolerance to rice. *Nature* **2006**, *442* (7103), 705−708.

(22) Bailey-Serres, J.; Fukao, T.; Ronald, P.; Ismail, A.; Heuer, S.; Mackill, D. Submergence tolerant rice: SUB1's journey from landrace tomodern cultivar. *Rice* **2010**, *3* (2−3), 138−147.

(23) Fukao, T.; Yeung, E.; Bailey-Serres, J. The submergence tolerance regulator SUB1A mediates crosstalk between submergence and drought tolerance in rice. *Plant Cell* **2011**, *23* (1), 412−427.

(24) Barding, G. A.; Fukao, T.; Beni, S.; Bailey-Serres, J.; Larive, C. K. Differential metabolic regulation governed by the rice SUB1A gene during submergence stress and identification of alanylglycine by ^{1}H NMR spectroscopy. *J. Proteome Res.* **2012**, *11*, 320−330.

(25) Ko, S.; Eliot, A. C.; Kirsch, J. F. S-Methylmethionine is both a substrate and an inactivator of 1-aminocyclopropane-1-carboxylate synthase. *Arch. Biochem. Biophys.* **2004**, *421* (1), 85−90.

(26) Menegus, F.; Lilliu, I.; Brambilla, I.; Bonfa, M.; Scaglioni, L. Unusual accumulation of S-methylmethionine in aerobic-etiolated and in anoxic rice seedlings: An H-1-NMR study. *J. Plant Physiol.* **2004**, *161* (6), 725−732.

(27) Ravanel, S.; Gakiere, B.; Job, D.; Douce, R. The specific features of methionine biosynthesis and metabolism in plants. *Proc. Natl. Acad. Sci. U.S.A.* **1998**, *95* (13), 7805−7812.

(28) Bourgis, F.; Roje, S.; Nuccio, M. L.; Fisher, D. B.; Tarczynski, M. C.; Li, C. J.; Herschbach, C.; Rennenberg, H.; Pimenta, M. J.; Shen, T. L.; Gage, D. A.; Hanson, A. D. S-methylmethionine plays a major role in phloem sulfur transport and is synthesized by a novel type of methyltransferase. *Plant Cell* **1999**, *11* (8), 1485−1497.

(29) Narsai, R.; Howell, K. A.; Carroll, A.; Ivanova, A.; Millar, A. H.; Whelan, J. Defining core metabolic and transcriptomic responses to oxygen availability in rice embryos and young seedlings. *Plant Physiol.* **2009**, *151* (1), 306−322.

(30) Goto, S.; Bono, H.; Ogata, H.; Fujibuchi, W.; Nishioka, T.; Sato, K.; Kanehisa, M. Organizing and computing metabolic pathway data in terms of binary relations. *Pac. Symp. Biocomputing '97* **1997**, 175−186186.

(31) Martinelli, T.; Whittaker, A.; Masclaux-Daubresse, C.; Farrant, J. M.; Brilli, F.; Loreto, F.; Vazzana, C. Evidence for the presence of photorespiration in desiccation-sensitive leaves of the C-4 "resurrection" plant Sporobolus stapfianus during dehydration stress. *J. Exp. Bot.* **2007**, *58* (14), 3929−3939.

(32) Dubos, C.; Huggins, D.; Grant, G. H.; Knight, M. R.; Campbell, M. M. A role for glycine in the gating of plant NMDA-like receptors. *Plant J.* **2003**, *35* (6), 800−810.

(33) De Silva, D. L. R.; Hetherington, A. M.; Mansfield, T. A. Synergism between calcium ions and abscisic acid in preventing stomatal opening. *New Phytol.* **1985**, *100* (4), 473−482.

(34) Subbaiah, C. C.; Sachs, M. M. Molecular and cellular adaptations of maize to flooding stress. *Ann. Bot.* **2003**, *91* (2), 119−127.

(35) Bailey-Serres, J.; Chang, R. Sensing and signalling in response to oxygen deprivation in plants and other organisms. *Ann. Bot.* **2005**, *96* (4), 507−518.
(36) Kumar, A.; Bachhawat, A. K. Pyroglutamic acid: Throwing light on a lightly studied metabolite. *Curr. Sci.* **2012**, *102* (2), 288−297.
(37) Schilling, S.; Stenzel, I.; von Bohlen, A.; Wermann, M.; Schulz, K.; Demuth, H. U.; Wasternack, C. Isolation and characterization of the glutaminyl cyclases from *Solanum tuberosum* and *Arabidopsis thaliana*: Implications for physiological functions. *Biol. Chem.* **2007**, *388* (2), 145−153.
(38) Bailey-Serres, J.; Voesenek, L. Flooding stress: Acclimations and genetic diversity. *Annu. Rev. Plant Biol.* **2008**, *59*, 313−339.
(39) Bailey-Serres, J.; Fukao, T.; Gibbs, D. J.; Holdsworth, M. J.; Lee, S. C.; Licausi, F.; Perata, P.; Voesenek, L. A. C. J.; van Dongen, J. T. Making sense of low oxygen sensing. *Trends Plant Sci.* **2012**, *17* (3), 129−138.
(40) Shelp, B. J.; Mullen, R. T.; Waller, J. C. Compartmentation of GABA metabolism raises intriguing questions. *Trends Plant Sci.* **2012**, *17* (2), 57−59.
(41) Sweetlove, L. J.; Beard, K. F. M.; Nunes-Nesi, A.; Fernie, A. R.; Ratcliffe, R. G. Not just a circle: Flux modes in the plant TCA cycle. *Trends Plant Sci.* **2010**, *15* (8), 462−470.
(42) Gross, J. H. *Mass Spectrometry*; Springer-Verlag: Berlin, 2004; p 507.
(43) Lombardo, V. A.; Osorio, S.; Borsani, J.; Lauxmann, M. A.; Bustamante, C. A.; Budde, C. O.; Andreo, C. S.; Lara, M. V.; Fernie, A. R.; Drincovich, M. F. Metabolic profiling during peach fruit development and ripening reveals the metabolic networks that underpin each developmental stage. *Plant Physiol.* **2011**, *157* (4), 1696−1710.
(44) Howell, K. A.; Narsai, R.; Carroll, A.; Ivanova, A.; Lohse, M.; Usadel, B.; Millar, A. H.; Whelan, J. Mapping metabolic and transcript temporal switches during germination in rice highlights specific transcription factors and the role of RNA instability in the germination process. *Plant Physiol.* **2009**, *149* (2), 961−980.
(45) Muhlemann, J. K.; Maeda, H.; Chang, C. Y.; San Miguel, P.; Baxter, I.; Cooper, B.; Perera, M. A.; Nikolau, B. J.; Vitek, O.; Morgan, J. A.; Dudareva, N. Developmental changes in the metabolic network of snapdragon flowers. *Plos One* **2012**, *7* (7), e40381.
(46) Wang, S. F.; Wang, X. F.; He, Q. W.; Liu, X. X.; Xu, W. L.; Li, L. B.; Gao, J. W.; Wang, F. D. Transcriptome analysis of the roots at early and late seedling stages using Illumina paired-end sequencing and development of EST-SSR markers in radish. *Plant Cell Rep.* **2012**, *31* (8), 1437−1447.
(47) Thurman, E. M.; Ferrer, I. Comparison of quadrupole time-of-flight, triple quadrupole, and ion-trap mass spectrometry/mass spectrometry for the analysis of emerging contaminants. In *Liquid Chromatography/Mass Spectrometry, MS/MS and Time of Flight MS*; American Chemical Society: Washington, DC, 2003; Vol. *850*, pp 14−31.
(48) Barding, G.; Salditos, R.; Larive, C. Quantitative NMR for bioanalysis and metabolomics. *Anal. Bioanal. Chem.* **2012**, *404* (4), 1165−1179.
(49) Kusano, M.; Tabuchi, M.; Fukushima, A.; Funayama, K.; Diaz, C.; Kobayashi, M.; Hayashi, N.; Tsuchiya, Y. N.; Takahashi, H.; Kamata, A.; Yamaya, T.; Saito, K. Metabolomics data reveal a crucial role of cytosolic glutamine synthetase 1;1 in coordinating metabolic balance in rice. *Plant J.* **2011**, *66* (3), 456−466.